



# VISTA INTERNATIONAL JOURNAL ON ENERGY, ENVIRONMENT & ENGINEERING



## How Measurement Noise Shapes Spatial Predictions: A Multi-distribution Analysis of Interpolation Sensitivity

Suddhasheel Ghosh

Department of Civil Engineering,  
Jawaharlal Nehru Engineering College, MGM University,  
Chhatrapati Sambhajinagar (M.S.), India

\*Corresponding Author's E-mail: sghosh@mgmu.ac.in Mob.: +91 7387183408

### ABSTRACT

Spatial interpolation is widely used in environmental modelling and geospatial analysis. Literature reveals that the understanding of propagation of measurement noise through the spatial interpolation algorithms, is still limited. In this study we investigate how additive noise following different statistical distributions viz. normal, lognormal, beta and gamma influence the interpolated predictions generated by Inverse Distance Weighting (IDW), Thin Plate Splines (TPS) and Ordinary Kriging (OK). We use the Meuse heavy-metal dataset, and perform Monte-Carlo simulations in which the measurements of Zinc are perturbed with random noise drawn from Normal, Lognormal, Beta and Gamma distributions, across of range of standard deviations. Using three selected locations which are located inside the convex hull of the location of observation, we calculate the interpolated values. The resulting ensembles are then analysed using the Kolmogorov-Smirnov goodness-of-fit tests to assess conformity to theoretical distribution models. The results show that IDW is most sensitive to local perturbations, whereas TPS demonstrated the most distribution preserving behaviour. Ordinary Kriging, on the other hand, balances local sensitivity with smoothing derived from the variogram structure. This study highlight the spatial dependence of noise propagations, as different neighbourhood characteristics yield very distinct statistical outcomes. Therefore, we obtain a structured framework for understanding uncertainty propagation in spatial interpolation and underline the importance of considering noise characteristics while interpreting interpolated surfaces.

**Keywords :** *Spatial Interpolation, Uncertainty propagation, Noise modelling, environmental geostatistics, Monte Carlo simulation.*



This article is an open access article distributed under the terms and conditions of the Creative Commons Attribution (CC BY) license (<https://creativecommons.org/licenses/by/4.0/>).

## 1. Introduction :

Spatial interpolation plays a central role in environmental modelling, hydrology, geostatistics, and geospatial decision-making, where observations are often limited to discrete point samples [1]. By generating continuous surfaces from sparse measurements, interpolation techniques enable the construction of pollution maps, soil quality assessments, hydrological surfaces, and risk estimation models. Despite their widespread application, interpolation outputs are rarely examined in terms of how they respond to uncertainty in the underlying measurements. Field observations in environmental studies are frequently affected by sampling errors, laboratory uncertainties, sensor noise, and small-scale environmental variability. These sources of uncertainty propagate into the interpolated surface, yet the magnitude and structure of this propagation remain poorly understood [2].

An important but often overlooked aspect is that measurement noise may not always follow the Gaussian assumptions typically made in error modeling [3]. Environmental variables such as heavy-metal concentrations, rainfall, or pollutant loads often exhibit skewness, heavy tails, and bounded behaviour, which are better described by non-Gaussian distributions such as Lognormal [4], Gamma [5], or Beta [6]. Understanding how such distributional characteristics influence interpolation outcomes is therefore crucial for robust spatial analysis.

Spatial interpolation techniques differ fundamentally in how they incorporate neighbourhood information. Inverse Distance Weighting (IDW) relies heavily on the nearest observations, Thin Plate Splines (TPS) apply global smoothing, and Ordinary Kriging (OK) leverages spatial autocorrelation structures through the variogram. These methodological differences suggest that each interpolator may respond uniquely to measurement noise. However, there has been limited systematic research quantifying how noise of different distributional forms affects the statistical behaviour of interpolated predictions.

This study addresses this gap by conducting a comprehensive Monte Carlo simulation [7] and subsequent analysis using the Meuse heavy-metal dataset [8]. Additive noise drawn from Normal, Lognormal, Beta, and Gamma distributions is imposed on the zinc concentrations, and the resulting interpolated predictions at selected spatial points are examined. By applying Kolmogorov–Smirnov goodness-of-fit tests [9] to the simulation outputs, the study provides new insights into the noise-to-output transformation properties of each interpolation method. This contributes to a deeper understanding of uncertainty propagation in spatial modelling and supports more informed methodological choices in environmental assessment and decision-making.

## 2. Literature Review :

Several earlier studies have investigated aspects of uncertainty in spatial interpolation, though typically in narrower contexts than considered here. Early geostatistical literature emphasized the role of kriging variance in representing prediction uncertainty, but this primarily reflects spatial configuration and model assumptions rather than measurement noise [10]. Journel et al. [11] and subsequent geostatistical works have acknowledged measurement error through the nugget effect, but without evaluating how different noise distributions affect predictions.

In the environmental sciences, a few studies have explored the influence of noise on interpolation accuracy or mapping outcomes, often using synthetic Gaussian noise to test robustness. Research on rainfall interpolation, air-quality mapping, and soil contamination surfaces has highlighted that IDW is highly sensitive to local perturbations [12], whereas smoothing-based approaches such as splines exhibit lower sensitivity. However, these studies typically focus on pointwise accuracy rather than distributional behaviour of predictions.

More recent work has examined the propagation of uncertainty in kriging models through Bayesian frameworks or conditional simulations, but these focus primarily on model-based uncertainty rather than measurement noise [13]. Similarly, studies on Monte Carlo approaches in spatial analysis often consider errors in variogram parameters or sampling design, rather than explicitly transforming measurement noise through the interpolation function [14].

It is to be imperatively noted that the existing literature provides very limited discussion on how non-Gaussian measurement noise—particularly skewed or bounded noise—affects interpolated outputs. Virtually no studies systematically compare multiple interpolation methods under diverse noise distributions using controlled Monte Carlo simulation. Therefore, this study fills a meaningful gap by evaluating how Normal, Lognormal, Beta, and Gamma noise propagate through IDW, TPS, and OK, and by assessing the resulting distributional transformations using formal goodness-of-fit testing.

## 2.1 Objectives of this study :

To fill the gap in the literature, we propose the following primary objective of this paper: To evaluate how additive measurement noise of different statistical forms propagates through commonly used spatial interpolation algorithms. Specifically, this paper will:

- a. Simulate measurement noise from four distribution families—Normal, Lognormal, Beta, and Gamma—across a range of standard deviations.
- b. Additively perturb the Meuse zinc concentrations and apply IDW, Thin Plate Splines, and Ordinary Kriging using a fixed variogram model.
- c. Generate Monte Carlo ensembles of interpolated predictions at selected spatial locations to capture the distributional variability induced by noise.
- d. Assess the resulting distributions using Kolmogorov–Smirnov goodness-of-fit tests for each noise scenario and interpolation method.
- e. Compare how different interpolation algorithms transform measurement uncertainty, identifying which methods amplify, smooth, or preserve distributional characteristics.

Together, these objectives provide a comprehensive framework for understanding uncertainty propagation in spatial interpolation.

## 3. Materials and Methods :

### 3.1 Study area and dataset :

The analysis is based on the well-known Meuse dataset, which documents heavy-metal concentrations in floodplain soils along the Meuse River in the Netherlands. The dataset consists of spatial point measurements collected at 155 locations, each recorded with precise x–y coordinates in the Dutch national RD New coordinate system (EPSG:28992). Among several heavy metals measured, zinc concentration is selected as the target variable due to its pronounced spatial variability and its long-standing use as a benchmark in geostatistical research. The spatial distribution of zinc values reflects both natural depositional processes and historical contamination patterns, making it a realistic test case for studying interpolation behaviour under uncertainty. The dataset is particularly suitable for methodological studies because of its moderate sample density, heterogeneity in concentration levels, and availability of an associated prediction grid. These characteristics collectively allow controlled experimentation on how synthetic noise modifies interpolation outputs while maintaining strong relevance to real-world environmental monitoring scenarios.

### 3.2 Addition of noise to data :

To investigate how measurement uncertainty influences spatial interpolation outcomes, random noise is added to the observed zinc concentrations in the Meuse dataset prior to interpolation. This noise is treated as an additive perturbation, reflecting common sources of variability such as field sampling errors, laboratory measurement imprecision, and short-range environmental fluctuations that are not captured by the spatial process. The additive error model is expressed as

$$Z_{\text{noisy}} = Z_{\text{observed}} + \varepsilon,$$

where  $\varepsilon$  is a random variable drawn from one of four candidate distributions. By systematically varying both the distributional form and the magnitude (standard deviation) of the noise, we aim to isolate how different types of uncertainty propagate through different spatial interpolation algorithms. We describe the Normal, Lognormal, Beta, and Gamma noise models follow in the subsequent subsections.

### 3.2.1 Normal noise :

The Normal distribution is the most widely used model for representing measurement error. When multiple small and independent sources of error contribute to the final measurement—such as sampling imprecision, instrument noise, and laboratory handling effects—the resulting uncertainty can often be approximated by a Gaussian distribution. In this study, Normal noise is added additively to the zinc concentrations, preserving the sign and allowing both positive and negative perturbations. The symmetry of the distribution implies that over repeated realizations, errors are equally likely to increase or decrease measured values. This property makes Normal noise a useful baseline for comparing the behaviour of interpolation algorithms, particularly in assessing whether they distort, preserve, or modify the underlying symmetry of the imposed uncertainty. Studying Normal noise also helps identify whether nonlinear transformations or distance-weighted methods introduce systematic skew or bias into interpolated predictions.

### 3.2.2 Lognormal noise :

The Lognormal distribution is frequently used to describe measurement errors in environmental and geochemical data, especially when uncertainties are multiplicative in nature. While the study implements an additive formulation for consistency across distributions, the Lognormal form still captures the characteristic right-skewed behaviour commonly observed in pollutant concentrations and trace-metal assays. In this model, the noise term is generated as a lognormally distributed random variable shifted appropriately so that it may be added directly to the observed zinc values. This ensures that the distribution retains its positivity and skew while conforming to the additive framework. Lognormal noise tends to produce occasional large positive deviations, reflecting real-world phenomena such as sporadic contamination hotspots or laboratory anomalies. These heavy-tailed characteristics make Lognormal noise especially useful for testing the robustness of interpolation algorithms, as IDW, TPS, and Kriging may respond differently to infrequent but substantial perturbations in local input values.

### 3.2.3 Beta noise :

The Beta distribution offers a flexible framework for modelling bounded measurement noise, making it particularly suitable when uncertainties are believed to lie within a finite range. In this study, the Beta distribution is used in a transformed form, where a standard Beta variate defined on the interval (0,1) is rescaled to match a symmetric range around the original zinc values. This allows the noise to remain bounded while still exhibiting a range of shapes—from uniform-like to highly skewed—depending on its parameters. Beta noise is especially relevant when measurement instruments have known operational limits, or when expert judgement suggests that extreme deviations are implausible. By imposing bounded noise, the study examines how interpolation algorithms behave when uncertainties cannot exceed a prescribed threshold. This provides insight into whether smoothing or distance-weighted methods clip, amplify, or preserve the bounded structure of the imposed perturbations.

### 3.2.4 Gamma noise :

The Gamma distribution is a versatile model for representing strictly positive, right-skewed uncertainties. It is commonly used in hydrology, environmental monitoring, and reliability analysis, where variability arises from processes

that accumulate over time or depend on multiplicative factors. In the context of this study, Gamma-distributed noise is shifted to ensure compatibility with the additive model while preserving its key features—positivity, skewness, and heavy right tail. Gamma noise introduces a higher likelihood of moderate-to-large upward perturbations compared to Gaussian noise, making it ideal for assessing how interpolation algorithms respond to asymmetric and heteroscedastic uncertainty.

### 3.3 Spatial Interpolation algorithms :

In this study we choose three easily implementable spatial interpolation algorithms – (a) inverse distance weighted method (IDW), (b) Thin Plate Splines, and (c) Ordinary Kriging. For all these interpolation algorithms, the natural logarithm of the observations of Zinc are used in our study. The details about these interpolation algorithms are given in the following subsections.

#### 3.3.1 Inverse distance weighting method :

Inverse Distance Weighting (IDW) is a deterministic spatial interpolation technique that estimates values at unsampled locations as a weighted average of nearby observations, where weights decrease with distance. In the standard form of this method, given points  $\mathbf{p}_i (x_i, y_i)$  and the observation values  $Z_i = Z(\mathbf{p}_i)$ , the predicted value at a location  $\mathbf{p}(x, y)$  is given by,

$$IDW(\mathbf{p}) = \frac{\sum_{i=1}^n w_i(\mathbf{p})Z(\mathbf{p}_i)}{\sum_{i=1}^n w_i(\mathbf{p})}, \text{ where } w_i(\mathbf{p}) = d(\mathbf{p}_i, \mathbf{p})^{-n} \quad (1)$$

where  $d(\mathbf{p}, \mathbf{p})$  is the Euclidean distance and  $n$  is the power parameter, typically set to 2. Because IDW assigns greater influence to observations closest to the prediction point, it is particularly sensitive to local fluctuations in the data. This property makes IDW highly responsive to additive measurement noise, as perturbations in nearby observations propagate directly and often disproportionately into the final interpolated value.

#### 3.3.2 Thin plate splines :

Thin Plate Splines (TPS) are a smooth, flexible interpolation technique based on the theory of radial basis functions. TPS constructs a continuous surface that minimizes the total “bending energy,” analogous to deforming an infinitely thin metal sheet so that it passes as closely as possible through the observed data points. The interpolated value at a location  $\mathbf{p}(x, y)$  is expressed as a weighted combination of radial basis functions of the form

$$U(r) = r^2 \log(r) \quad (2)$$

where  $r$  is the Euclidean distance to each observation, along with a polynomial term that ensures global smoothness. This formulation allows TPS to capture broad spatial trends while dampening high-frequency noise.

#### 3.3.3 Ordinary kriging :

Ordinary Kriging (OK) is a geostatistical interpolation method that models spatial variation through an explicit representation of spatial autocorrelation. Unlike deterministic techniques such as IDW or spline-based approaches, Kriging is grounded in the theory of random fields and assumes that the underlying spatial process exhibits second-order stationarity with a constant but unknown mean. The key component of OK is the semivariogram, which quantifies how similarity between observations decreases with increasing separation distance. In this study, a fixed variogram model—fitted to the log-transformed zinc concentrations—is used across all simulations to ensure that differences in

interpolated outputs arise solely from the imposed measurement noise and not from changes in the spatial correlation structure.

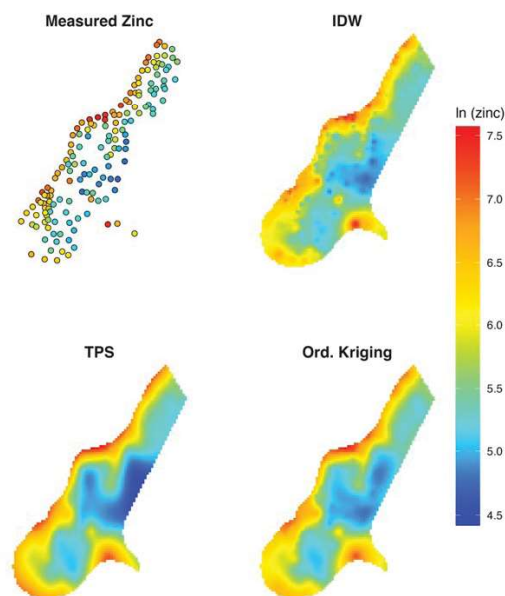


**Fig.1.** Outputs of the IDW, TPS and Ordinary Kriging interpolations

The outputs of the IDW, TPS and Ordinary Kriging interpolations for log *Zinc* are presented in Fig.1.

### 3.4 Monte carlo simulation approach :

The Monte Carlo experiment is designed to quantify how additive measurement errors of varying distributional forms propagate through spatial interpolation algorithms. Each simulation begins with the generation of synthetic noise using one of four random number generators—Normal, Lognormal, Beta, or Gamma—implemented through custom functions that allow precise control over the mean and standard deviation. This noise is added to the original zinc concentrations ( $Z$ ) in the Meuse dataset, following the additive model  $Z_{\text{noisy}} = Z + \varepsilon$ . Because interpolation is performed on the log-transformed variable, the noisy concentrations are transformed to  $\log(Z_{\text{noisy}})$  prior to interpolation.

For each noise realization, predictions at three fixed locations are computed using IDW, Thin Plate Splines, and Ordinary Kriging, the last of which employs a fixed variogram model derived from the log-transformed zinc values. Back-transformation to the original concentration scale is performed using the naive exponential transform for IDW and TPS, and a bias-corrected transform for Kriging based on the estimated prediction variance. The entire procedure is repeated 1,000 times for each distribution–standard deviation combination using parallel computation to ensure scalability and reproducibility.

#### 3.4.1 Choice of the three fixed locations :

To assess how additive measurement errors propagate through different interpolation algorithms, the study evaluates interpolated values at three spatially distributed prediction points. These points are generated uniformly at random within the convex hull formed by the Meuse sampling locations, ensuring that interpolation is performed strictly within the region supported by actual data and avoiding the instability associated with extrapolation. The convex hull provides a mathematically well-defined spatial boundary that captures the full extent of observed zinc concentrations while maintaining geometric simplicity. Sampling points uniformly within this region ensures that no directional or spatial bias influences the assessment of interpolation error propagation. By selecting three distinct locations, the analysis

captures the variability in predictions arising from local neighbourhood structure, spatial gradients, and differing distances to sampled points. These prediction points remain fixed for all Monte Carlo replicates, allowing direct comparison of distributional outcomes across noise distributions and interpolation methods.

### 3.4.2 Hypothesis testing for goodness of fit using Kolmogorov-Smirnov test :

The Kolmogorov–Smirnov (KS) test is employed to quantitatively assess how well the predicted values at each interpolation point conform to the Normal, Lognormal, Beta, and Gamma distributions. The KS test compares the empirical cumulative distribution function (ECDF) of the simulated predictions with the theoretical cumulative distribution function (CDF) corresponding to each candidate distribution. The test statistic is defined as the maximum absolute difference between the ECDF and the fitted CDF, providing a non-parametric and distribution-free measure of discrepancy. Parameter estimation for each family is carried out prior to testing: mean and standard deviation for the Normal, log-scale parameters for the Lognormal, shape parameters for the Beta (after rescaling to a unit interval), and shape–rate parameters for the Gamma distribution.

**Parameter estimation** - Accurate parameter estimation is essential for evaluating goodness-of-fit using the Kolmogorov–Smirnov test, as the theoretical distribution must closely reflect the characteristics of the simulated predictions. For the Normal distribution, parameters are estimated using the sample mean and sample standard deviation of the predicted values. The Lognormal distribution is fitted by transforming the data to the logarithmic scale and computing the mean and standard deviation of the log-transformed values, which define the corresponding lognormal parameters. The Beta distribution, defined on the interval (0,1), requires rescaling the predictions to this unit range. Initial shape parameters are obtained through method-of-moments estimates, and when these are unstable or invalid, a maximum-likelihood optimisation is performed to refine the shape parameters. For the Gamma distribution, method-of-moments estimates of shape and rate parameters are first computed using the sample mean and variance, and subsequently refined using numerical maximum-likelihood estimation where appropriate. These estimation procedures ensure that each theoretical distribution is tailored to the empirical characteristics of the interpolated predictions, thereby enabling a consistent and meaningful application of the KS test across all noise scenarios and interpolation methods.

The resulting KS p-values indicate the plausibility of each distributional assumption, with smaller values (typically  $p < 0.05$ ) suggesting that the observed sample of predictions is unlikely to originate from the fitted theoretical distribution. By applying the KS test consistently across all noise scenarios and interpolation methods, we systematically evaluate how interpolation transforms, preserves, or distorts the statistical structure of measurement errors.

### 3.5 Hardware and software used :

The work done in this paper is achieved using the R software [15] and its packages viz. *gstat* [16,17], *sp* [18], and *fitdistrplus* [19]. The Monte-Carlo simulation is facilitated by the *doParallel* [20] and *foreach* [21] packages. We use a MacBook Pro M1 laptop with 16GB RAM for the computations.

## 4. Results and discussion :

Monte-Carlo simulation results are discussed in the following subsections.

### 4.1 Monte-Carlo simulation :

During the Monte-Carlo simulation process, we generate random noise using four customised random number generators for control over mean and standard deviation. While we fixed the mean at 0, we chose the standard deviations from the set {0.1, 0.2, 0.5, 0.75, 1.0, 1.25, 1.5, 1.75, 2}. For each combination of the random number generator and

standard deviation, 1000 simulations are done for (a) generation of random additive noise, (b) interpolating the noisy data over the three fixed points, and calculating the resultant values. Therefore, in all  $4 \times 9 \times 1000 = 36000$  simulations were run for interpolating the values of natural logarithm of the measured variable using IDW, TPS and Ordinary Kriging.

The collection of resultant values for each of the points is then evaluated for the goodness of fit using the KS test for normal, lognormal, beta and gamma distributions. In Fig. 2, Fig. 3, Fig. 4, and Fig. 5 we showcase the outputs for the input standard deviation = 0.75, and for the respective random number generators for normal, lognormal, beta and gamma distributions. The figures are annotated with the p-values obtained from the KS tests, and indicate the goodness of fit for normal, lognormal, beta and gamma distributions respectively. As was mentioned earlier, p values which are less than 0.05, indicate that the particular distribution does not fit to the results of the simulation. The p-values of the KS test are summarized in Table 1. The cases where the KS-test rejects the null hypothesis (the data does not belong to the distribution) are marked in italicised text.

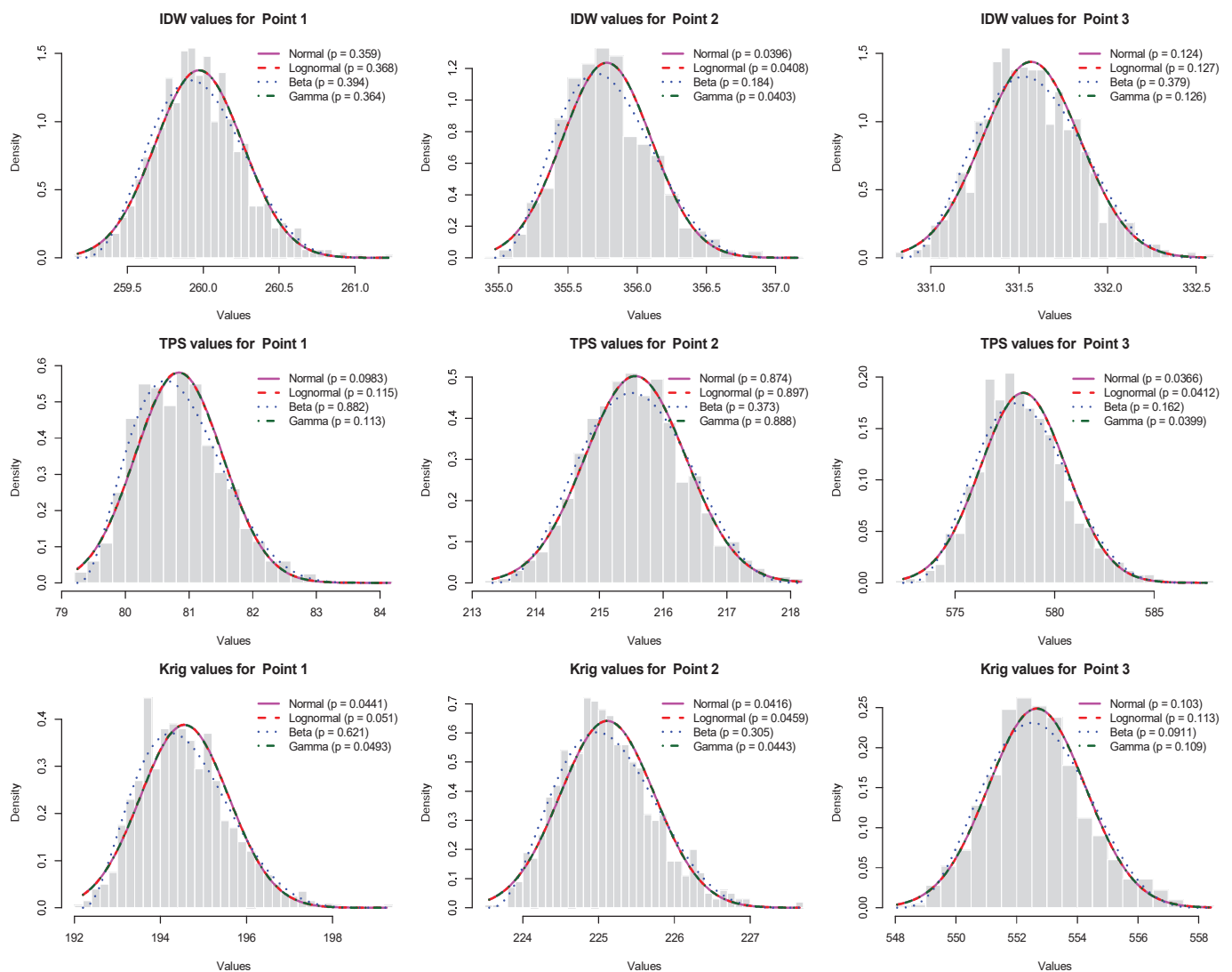


**Fig. 1.** Histograms and curve fits when the standard deviation is 0.75 with a normal noise

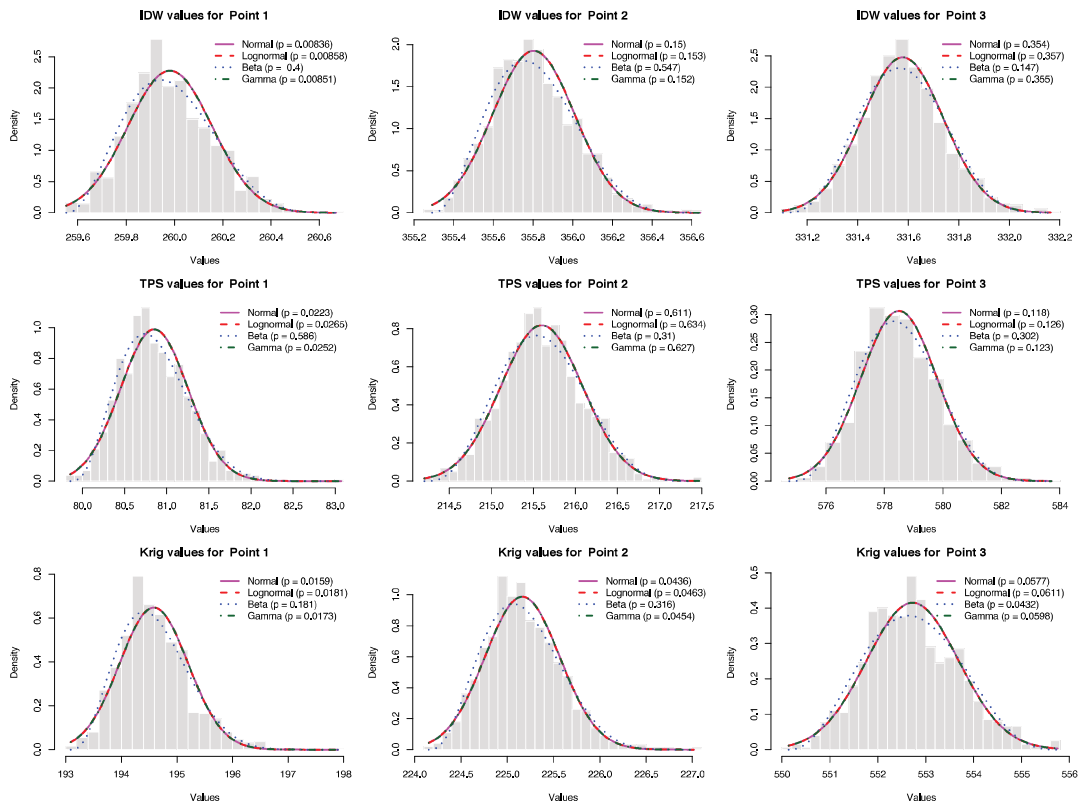


Fig. 2. Histograms and curve fits when the standard deviation is 0.75 with lognormal noise

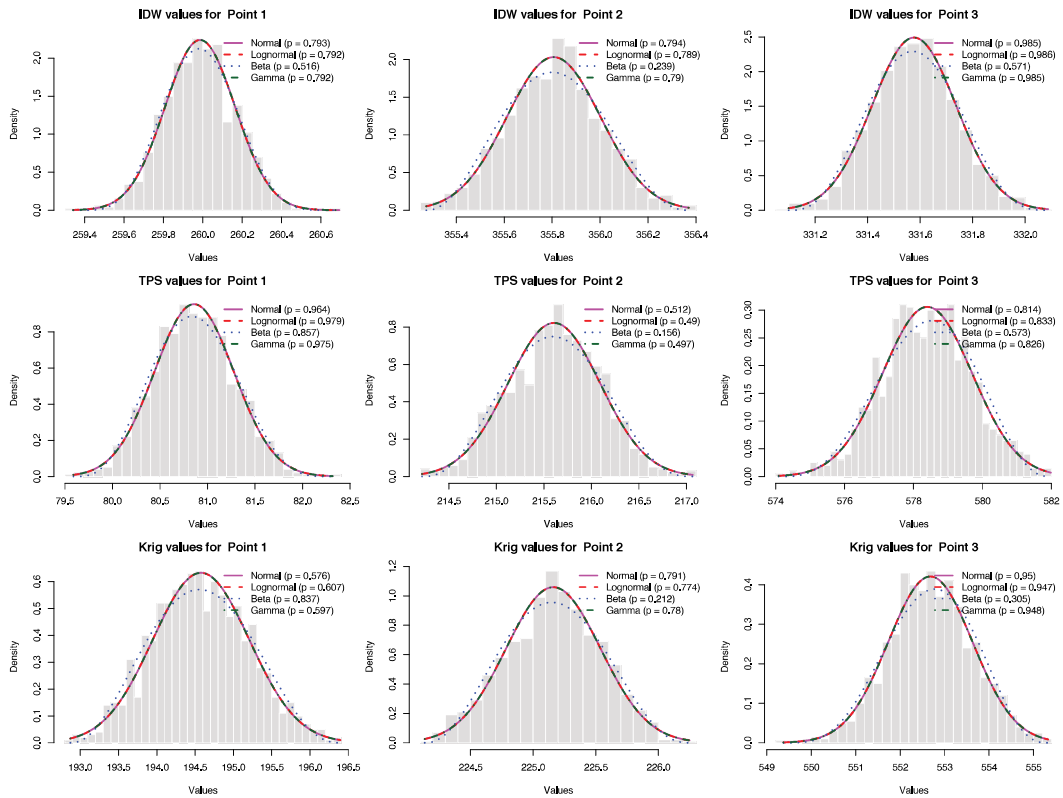


Fig. 3. Histograms and curve fits when the standard deviation is 0.75 with beta noise

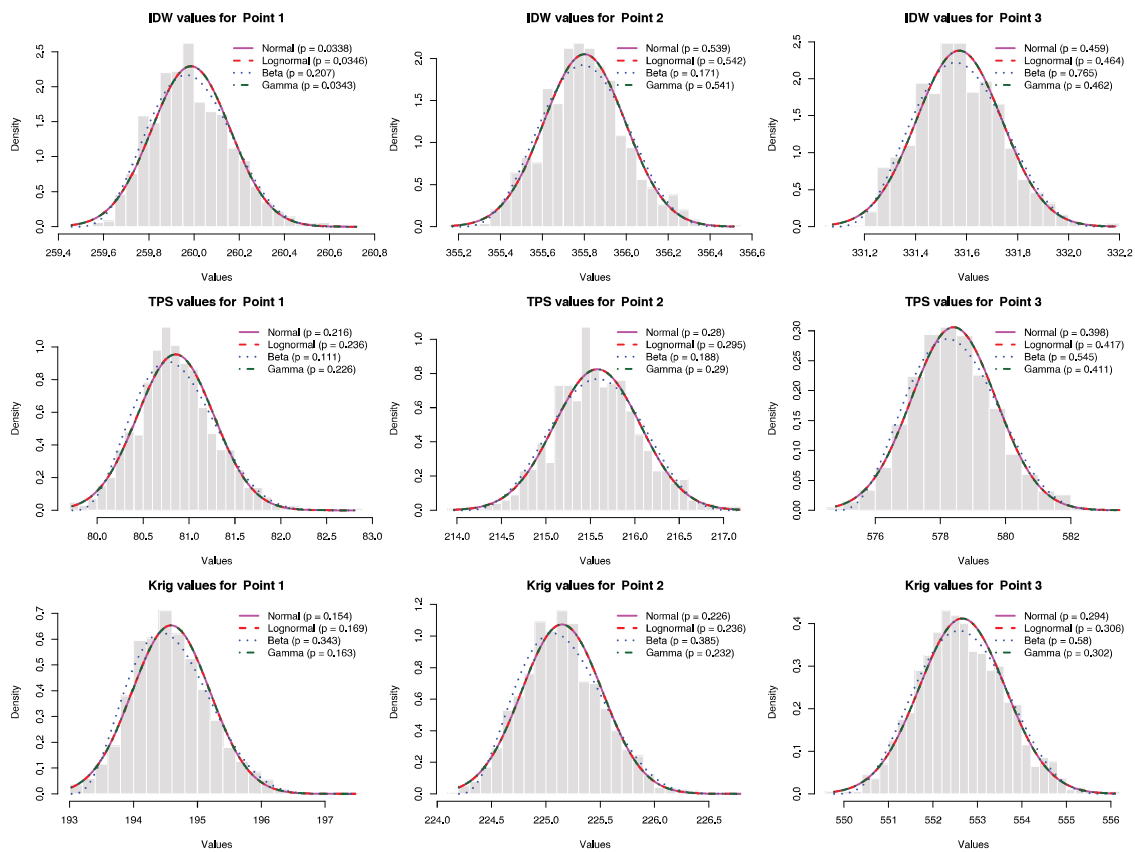


Fig. 4. Histograms and curve fits when the standard deviation is 0.75 with gamma noise

#### 4.2 Observations from the graphs and table :

From the plotted graphs which correspond to the different input noise distributions (see Fig. 2, Fig. 3, Fig. 4, and Fig. 5), we observe that in all the cases, the fitted curve is like a bell curve, just like the normal distribution. Where the input noise is lognormal, the fitted curves to the histogram of interpolated output values are skewed to the right. On the other hand, for the beta distributed noise, the curves appear symmetrical. The right skewed behaviour is also observed for the gamma distributed noise.

The goodness-of-fit results at a noise standard deviation of 0.75 reveal clear and consistent patterns in how the three interpolation algorithms—IDW, Thin Plate Splines (TPS), and Ordinary Kriging (OK)—transform different forms of input uncertainty. Across all noise scenarios and prediction points, TPS consistently produces the highest p-values, indicating that the interpolated values closely follow the assumed distribution of interest. This behaviour is expected given the smoothing nature of TPS, which reduces local variability and tends to yield prediction distributions that are more regular and less influenced by extreme perturbations. In contrast, IDW frequently produces the lowest p-values, reflecting its sensitivity to local fluctuations and its tendency to preserve or even amplify the skewness or irregularity introduced by the noise.

**Table 1.** p-values of the Kolmogorov-Smirnov (KS) test for fitting into normal, lognormal, beta and gamma distributions, for input noise in different random number generators in different distributions.

	Pt ID	Input noises with standard deviation as 0.75 for different random number generators											
		Normal			Lognormal			Beta			Gamma		
		IDW	TPS	OK	IDW	TPS	OK	IDW	TPS	OK	IDW	TPS	OK
Normal	1	0.3590	0.9830	0.0441	0.0080	0.0223	0.0159	0.7930	0.9640	0.5760	0.3380	0.2160	0.1540
	2	0.0396	0.0874	0.0416	0.1500	0.6110	0.0459	0.7940	0.5120	0.7910	0.5390	0.2800	0.2260
	3	0.1240	0.0366	0.1030	0.3540	0.1180	0.0577	0.8140	0.8140	0.9500	0.4590	0.3980	0.2940
Lognormal	1	0.0368	0.0408	0.1270	0.0086	0.0265	0.0181	0.7920	0.9790	0.6070	0.0346	0.2360	0.1690
	2	0.1150	0.8970	0.0412	0.1530	0.6340	0.0463	0.7890	0.4900	0.7740	0.5420	0.2950	0.2360
	3	0.0510	0.0459	0.1130	0.3570	0.1260	0.0611	0.9860	0.8330	0.9470	0.4640	0.4170	0.3060
Beta	1	0.3940	0.8820	0.6210	0.4000	0.5860	0.1810	0.5160	0.8570	0.8370	0.2070	0.1110	0.3430
	2	0.1840	0.3730	0.3050	0.5470	0.3100	0.3160	0.2390	0.1560	0.2120	0.1710	0.1880	0.3850
	3	0.3790	0.1620	0.0911	0.1470	0.3020	0.0432	0.5710	0.5730	0.3050	0.7650	0.5450	0.5800
Gamma	1	0.0364	0.1130	0.0493	0.0085	0.0252	0.0173	0.7920	0.9750	0.5970	0.0343	0.2260	0.1630
	2	0.0403	0.8880	0.0443	0.1520	0.6270	0.0454	0.7900	0.4970	0.7800	0.5410	0.2900	0.2320
	3	0.1250	0.0399	0.1090	0.3550	0.1230	0.0598	0.9850	0.8260	0.9480	0.4620	0.4110	0.3020

For inputs generated from the Normal distribution, TPS yields p-values close to or above 0.90 at most points, while IDW occasionally produces marginal fits (e.g.,  $p \approx 0.04$ – $0.12$ ), and OK yields mixed results, with some low p-values around 0.04. This suggests that Normal noise propagates stably through TPS but becomes distorted under IDW and, to a lesser extent, OK.

When the Lognormal noise is introduced, the effect of right-skewness becomes evident. IDW and OK frequently return low to moderate p-values, particularly at Point 1, while TPS again displays relatively stable fits. The pattern indicates that Lognormal noise tends to be smoothed by TPS but interacts nonlinearly with the distance-weighted and covariance-based mechanisms of IDW and OK.

The Beta noise, representing bounded uncertainty, shows the most uniformly high p-values across all methods and points, particularly for TPS and OK. Even IDW returns moderate to strong fits (e.g.,  $p \approx 0.20$ – $0.57$ ). This suggests that bounded noise is less likely to be structurally distorted by the interpolation process, especially when the noise distribution itself is already constrained.

Finally, the Gamma noise results mirror those of the Lognormal case, with TPS again showing strong fits and IDW showing weaker ones. OK sits between the two, with reasonable but not uniformly strong p-values. This reinforces the view that interpolation behaves differently when the noise contains significant right-tail behaviour.

Overall, these results demonstrate that TPS is the most distribution-preserving method, IDW is the most distortion-prone, and OK provides an intermediate degree of transformation, consistent with theoretical expectations about smoothing, distance-weighting, and covariance-driven interpolation.

### 4.3 Spatial dependence of noise propagation :

An important observation from the goodness-of-fit results is that the distributional behaviour of the interpolated predictions varies noticeably across the three selected evaluation points, even though all simulations use the same noise distribution and variance. This phenomenon arises from the inherently spatial nature of interpolation, where predictions depend not only on the values of neighbouring observations but also on their geometric configuration around each target location.

Each prediction point lies within a distinct local neighbourhood characterized by differing densities of sample

points, varying distances to the nearest observations, and unique orientations relative to spatial gradients in zinc concentrations. IDW, TPS, and Ordinary Kriging use these spatial relationships to compute prediction weights, meaning that identical noise inputs do not propagate uniformly across the domain. Points situated near areas of high local variability tend to experience amplified effects of noise, whereas points in smoother regions inherit a more dampened response.

Furthermore, method-specific characteristics interact with the local neighbourhood. IDW, with its strong dependence on the nearest observations, is especially sensitive to local geometric irregularities. TPS spreads influence more globally, but its smoothing properties respond differently depending on local curvature. Kriging incorporates the underlying variogram structure, and prediction variance varies spatially depending on observation density and covariance relationships. Consequently, each prediction point yields a distinct empirical distribution of simulated values.

Because the Kolmogorov–Smirnov test evaluates the fit between these point-specific empirical distributions and theoretical models, the resulting p-values naturally differ across the three points. These differences highlight the crucial role of spatial context in shaping how measurement noise is filtered, amplified, or transformed by interpolation algorithms.

#### 4.4 Summary of discussion :

In this paper, we have seen that the results provide a comprehensive view of how additive measurement uncertainty interacts with spatial interpolation algorithms and how different noise distributions propagate through the interpolation process. The Monte Carlo simulations reveal that the sensitivity of interpolated predictions to input noise varies significantly among the three methods evaluated—IDW, Thin Plate Splines (TPS), and Ordinary Kriging (OK). IDW consistently exhibits the greatest susceptibility to noise, producing prediction distributions that frequently diverge from the assumed forms, especially under skewed or heavy-tailed noise such as Lognormal and Gamma. This behaviour arises from IDW's strong reliance on the nearest data points, which causes local perturbations to translate directly into prediction variability.

It is seen from the figures and the table that TPS demonstrates the opposite tendency, acting as the most distribution-preserving method across the study. Its inherent smoothing mechanism dampens local fluctuations and generates predicted values that align closely with the theoretical distributions, even when the input noise is strongly asymmetric. OK displays intermediate characteristics: it moderates noise effects through the spatial covariance structure yet retains sensitivity to local variability, particularly in regions with sparse sampling or strong spatial gradients.

The discussion also highlights the spatial dependence of noise propagation, as prediction points located in different neighbourhoods exhibit distinct empirical distributions and therefore different goodness-of-fit results. Therefore, we can say that interpolation error is not only a function of noise characteristics but also of local data geometry and the spatial structure of the underlying field. We have demonstrated through this analysis that the combined influences of noise distribution, noise magnitude, interpolation method, and spatial position collectively shape the statistical behaviour of interpolated predictions. These findings underscore the value of explicit noise propagation studies in environmental and geospatial modelling.

#### 5. Conclusion :

In this study, we have systematically examined how additive measurement errors of different distributional forms propagate through three easily implementable methods viz. IDW, TPS and Ordinary Kriging. We used controlled Monte-Carlo simulations based on the meuse dataset available with the gstat package of R, and the analysis of the outputs indicate the fundamental difference in how, uncertainty is transformed. Based on the analysis, IDW amplifies local noise, TPS dampens it and Ordinary Kriging has a balanced behaviour depending upon the spatial covariance

of the data. Therefore, the distribution of the predicted values at the fixed points depends both on the imposed noise and the local spatial configuration of sampling locations.

The applications of Kolmogorov-Smirnov goodness-of-fit tests tells us that TPS consistently preserves the underlying noise distributions. On the other hand, IDW exhibits the greatest susceptibility to distortion, especially where noise models are skewed. We see that Kriging's response is intermediate owing to the interplay between variogram-based smoothing and local neighbourhood structure. Therefore, it can be said that these findings highlight the importance of considering the characteristics of measurement error when interpreting interpolation outputs in environmental modelling, pollution mapping and geospatial decision making.

This study has provided us a rigorous framework for understanding and quantifying how uncertainty propagates across different interpolation methods. It has emphasised that robust spatial analysis should account for both the nature of measurement noise and the spatial mechanics of the chosen interpolation method.

### References :

- [1] Janssen S, Dumont G, Fierens F, Mensink C. Spatial interpolation of air pollution measurements using CORINE land cover data. *Atmospheric Environment*. 2008 June 1;42(20):4884–903.
- [2] Phillips DL, Marks DG. Spatial uncertainty analysis: propagation of interpolation errors in spatially distributed models. *Ecological Modelling*. 1996 Nov 15;91(1):213–29.
- [3] Guo Y, Shen Y, Tan J. Stochastic resonance in a piecewise nonlinear model driven by multiplicative non-Gaussian noise and additive white noise. *Communications in Nonlinear Science and Numerical Simulation*. 2016 Sept 1;38:257–66.
- [4] Griffith DA, Chun Y. Soil Sample Assay Uncertainty and the Geographic Distribution of Contaminants: Error Impacts on Syracuse Trace Metal Soil Loading Analysis Results. *International Journal of Environmental Research and Public Health*. 2021 Jan;18(10):5164.
- [5] Adam AM, Farouk RM, El-Desouky BS. Generalized gamma distribution for biomedical signals denoising. *SIViP*. 2023 Apr 1;17(3):695–704.
- [6] Zhang S, Zhou T, Sun L, Liu C. Kernel Ridge Regression Model Based on Beta-Noise and Its Application in Short-Term Wind Speed Forecasting. *Symmetry*. 2019 Feb;11(2):282.
- [7] Barbu A, Zhu S-C. *Monte Carlo Methods* [Internet]. Singapore: Springer; 2020 [cited 2025 Nov 24]. Available from: <http://link.springer.com/10.1007/978-981-13-2971-5>
- [8] Middelkoop H. Heavy-metal pollution of the river Rhine and Meuse floodplains in the Netherlands. *Netherlands Journal of Geosciences*. 2000 Dec 1;411–27.
- [9] Smirnov N. Table for Estimating the Goodness of Fit of Empirical Distributions. *The Annals of Mathematical Statistics*. 1948 June;19(2):279–81.
- [10] Loquin K, Dubois D. Kriging and Epistemic Uncertainty: A Critical Discussion. In: Jeansoulin R, Papini O, Prade H, Schockaert S, editors. *Methods for Handling Imperfect Spatial Information* [Internet]. Berlin, Heidelberg: Springer; 2010 [cited 2025 Nov 24]. p. 269–305. Available from: [https://doi.org/10.1007/978-3-642-14755-5\\_11](https://doi.org/10.1007/978-3-642-14755-5_11)
- [11] Journel AG, Journel AG, Huijbregts CJ. *Mining Geostatistics*. Blackburn Press; 2003. 616 p.
- [12] Bronowicka-Mielniczuk U, Mielniczuk J, Obroślak R, Przystupa W. A Comparison of Some Interpolation Techniques for Determining Spatial Distribution of Nitrogen Compounds in Groundwater. *Int J Environ Res*. 2019 Aug 1;13(4):679–87.

- [13] Song JJ, Kwon S, Lee G. Incorporation of parameter uncertainty into spatial interpolation using Bayesian trans-Gaussian kriging. *Adv Atmos Sci*. 2015 Mar 1;32(3):413–23.
- [14] Acosta J, Vallejos R, García-Soidán P. A penalized estimation of the variogram and effective sample size. *Spatial Statistics*. 2025 Oct 1;69:100921.
- [15] R Core Team. R: A Language and Environment for Statistical Computing [Internet]. Vienna, Austria: R Foundation for Statistical Computing; 2025. Available from: <https://www.R-project.org/>
- [16] Gräler B, Pebesma E, Heuvelink G. Spatio-Temporal Interpolation using gstat. *The R Journal*. 2016;8(1):204–18.
- [17] Pebesma EJ. Multivariable geostatistics in S: the gstat package. *Computers & Geosciences*. 2004;30:683–91.
- [18] Pebesma EJ, Bivand R. Classes and methods for spatial data in R. *R News*. 2005 Nov;5(2):9–13.
- [19] Delignette-Muller ML, Dutang C. fitdistrplus: An R Package for Fitting Distributions. *Journal of Statistical Software*. 2015;64(4):1–34.
- [20] Corporation M, Weston S. doParallel: Foreach Parallel Adaptor for the ‘parallel’ Package [Internet]. 2022. Available from: <https://CRAN.R-project.org/package=doParallel>
- [21] Microsoft, Weston S. foreach: Provides Foreach Looping Construct [Internet]. 2022. Available from: <https://CRAN.R-project.org/package=foreach>